Anal. Bioanal. Electrochem., Vol. 14, No. 7, 2022, 696-714

Analytical & Bioanalytical Electrochemistry

2022 by CEE
www.abechem.com

Full Paper

Highly Enhanced Electrochemical Performance of $LiNi_{0.5}Co_{0.2}Mn_{0.3}O_2$ by Surface Coating with Li-Ti-O Nanoparticles for Lithium-Ion Batteries

Hamed Pourfarzad,[1] Meysam Karimi,[2] Mohammad Saremi,[3] and Ramin Badrnezhad,[4,*]

[1]*Department of Analytical Chemistry, Faculty of Chemistry, University of Kashan, Kashan, P.O. Box 15875-4413, Iran*

[2]*Department of Material Engineering, University of Tehran, Tehran, P.O. Box 14115-175, Iran*

[3]*Department of Electrical Engineering, College of Technical and Engineering, West Tehran Branch Islamic Azad University, Tehran, Iran*

[4]*Department of Chemistry and Chemical Engineering, Malek-Ashtar University of Technology, Tehran, P.O. Box 15875-1774, Iran*

*Corresponding Author, Tel.: +989393939207

E-Mail: Badrnezhad@yahoo.com

Received: 20 May 2022 / Received in revised form: 22 June 2022 / Accepted: 8 July 2022 / Published online: 31 July 2022

Abstract- The Li-Ti-O-coated $LiNi_{0.5}Co_{0.2}Mn_{0.3}O_2$ (LTO@NCM) cathode materials are synthesized *via* an *in situ* co-precipitation method followed by the lithiation process and thermal annealing. The Li-Ti-O coating layer is designed to strongly adhere to the core-material with diffusion pathways for Li^+ ions. Measurements and analysis of structure, morphology and electrochemical properties have been applied. X-ray diffraction patterns showed the existence and conversion of lithium titanium oxide (Li-Ti-O labeled as LTO). Electrochemical tests suggest that compared with pristine NCM, The LTO layer works both as an excellent Li ion conductive layer and as a protective coating layer against the attack of HF in the electrolyte, and remarkably improves the cycling performance at higher charged state and rate capability of the LTO@NCM composite material. 3.0 *wt*.% LTO-coated NCM (LTO3) material exhibited higher capacity retentions of 94.8% than that of the bare one (58.2%) and nickel-riched cathodes (90-91%) after 100 cycles at cut-off charge voltages of 4.3V at 1C rate.

Keywords- Lithium-ion batteries; NCM Cathode material; Lithium titanium oxide layer, Surface Coating, Lithiation process; Thermal annealing

1. INTRODUCTION

Lithium-ion batteries have been used in many fields, such as electric vehicles, hybrid vehicles and large-scale energy storage systems [1-3]. However, with the development of society, our goal is to reach a driving range of 300 miles, which means that the specific energy of batteries is required to reach 250 Wh kg^{-1} per cell [4,5]. This is a large challenge for currently commercialized LIBs cathode materials such as $LiFePO_4$, $LiCoO_2$ and $LiMn_2O_4$, which cannot satisfy the requirements of high energy density. In the other side, Ni- layered oxides such as $LiNi_{0.5}Co_{0.2}Mn_{0.3}O_2$ are promising cathode candidates for lithium-ion batteries because of their high discharge capacity, high energy density, low toxicity and low cost for industrial applications [6]. However, the Ni- cathode materials still present many problems that need to be solved. First, due to the similar ionic radius of Ni^{2+} (0.69 Å) and Li^+ (0.76 Å), 3b lithium sites can be occupied by Ni^{2+} ions in the Li slab, leading to irreversible structure transition. Furthermore, Ni^{2+} ions have shown electrostatic interaction with the migrating Li^+, causing a poor lithium ion transport rate [7]. Second, thermal instability of $LiNi_{0.5}Co_{0.2}Mn_{0.3}O_2$, especially at high operating voltages (~4.6 V) and high temperatures (+55 °C), have hindered its widespread application because the nickel ions undergo side reactions with the electrolyte at high charge voltage and high temperature during the cycling. The Ni- cathode will transform from an R-3m layer structure to a spinel structure and then to a rock-salt structure. Such irreversible structure transitions lead to sluggish Li^+ diffusion kinetics and poor electrochemical cyclic performance [8-10]. Third, the surface lithium residuals (Li_2O/LiOH) are sensitive to moisture and transform to Li_2CO_3, which will hinder the Li^+ diffusion and reduce the capacity. Therefore, it is necessary to improve the interfacial stability between the electrode and the electrolyte to achieve the long-term stability and meet the safety requirements [11,12].

In recent years, there are many tactics to solve the above problems, including surface modification [13], doping [14], gradient material [15], binder modification [16] and separators modification [17]. Surface coating is one of the most effective strategies to overcome these problems [18]. The coating materials themselves can serve as different roles including physical protection barrier, electron conductive media, ionic conductive media or HF scavenger [19]. Among these materials, metal oxides such as Al_2O_3 [20], CuO [21], TiO_2 [22] and AlF_3 [23] or lithium metal oxides are the simplest and most common ones due to their numerous merits, and have been widely studied and applied in industrial products [24,25]. However, most of these coating materials, especially oxides, can hardly offer tunnels for Li-ion mobility during cycling also suffer from poor conductivity. An ideal coating material should act not only as a protective layer but also as a Li-ion conductor. Recently, ternary Li-Ti-O oxides, consisting of various stoichiometric and nonstoichiometric compounds, have been reported as promising materials for surface-modifying electrode materials [26,27]. These compounds, in addition to providing additional sites for the insertion of lithium ions, increase the diffusion coefficient of lithium ions in the cathodic structure [28]. In addition to acting as a protective layer against the electrolyte, these materials also create a three-dimensional path for lithium ions to move during the charging and discharging process, which

improves the electrochemical performance of the cathode material. The components of the Li_2O-TiO_2 system consist of four stable phases Li_4TiO_4, Li_2TiO_3, $Li_4Ti_5O_{12}$ and $Li_2Ti_3O_7$ and a semi-stable phase. $Li_4Ti_5O_{12}$ is one of the most promising compounds for coating cathodic materials that are expected to improve their electrochemical properties. This compound does not show any dimensional changes during the charge-discharge process and the insertion / desertion of lithium ions from its structure, which is called strain-free material, but its electrical conductivity is weak and about 10^{-13} $S.cm^{-1}$, which limits the full capacity at high charge-discharge rates and also reduces the diffusion coefficient of lithium ions. Therefore, high-capacity rate performance is not expected from this material. Li_2TiO_3 has a layered structure consisting of alternating layers of lithium and $LiTi_2$. This material shows moderate ionic conductivity and does not change dimensions during charge-discharge, so it is called non-strain material [29]. The electrical conductivity of Li_2TiO_3 is weak (10^{-11} $S.cm^{-1}$), which hinders the performance of Li_2TiO_3 material at high rates. Among the titanate compounds, the $Li_2Ti_3O_7$ compound has received the most attention due to its capacity of 175 mAh / g at 20 / C. $Li_2Ti_3O_7$ also has one of the highest equilibrium capacities reported for anodes with a voltage of 1.5 V with the insertion of approximately 2.24 mol lithium per mol of $Li_2Ti_3O_7$ [22,30]. The intercalation of lithium into the structure of this material is well reversible due to its very small dimensional changes (less than 2%) during the insertion/desertion process. $Li_2Ti_3O_7$ is also known as one of the fast ionic conductors due to its fully open and fully closed orthorombic structure. The average value of lithium-ion diffusion coefficient in $Li_2Ti_3O_7$ at 1.5 V is equal to 2×10^{-8} $cm^2.s^{-1}$ is measured which is much higher than the diffusion coefficient of lithium ions within $Li_4Ti_5O_{12}$ which is equal to 3×10^{-12} $cm^2.s^{-1}$. This excellent ionic conductivity is due to the $Li_2Ti_3O_7$ Ramsdelite framework, which provides empty or semi-empty pathways for the incorporation of lithium ions [31,32]. Also, the electrical conductivity of $Li_2Ti_3O_7$ at room temperature is 4.05×10^{-7} $S.cm^{-1}$. Therefore, the compound $Li_2Ti_3O_7$ is considered as a material with full electrical conductivity [33]. Therefore, as a result, the properties of $Li_2Ti_3O_7$ are superior to other lithium compounds Li-Ti-O oxides. But $Li_2Ti_3O_7$ has not yet been coated on any cathode, although it has better ionic conductivity than other lithium titanate compounds. On the other hand, the theoretical capacity of this compound is more than others and due to small dimensional changes during the charge-discharge process, it has shown good cyclicity when tested as an anode. It also acts as an electrochemical inert layer at voltages above 1.5 V inside the organic electrolyte and prevents direct contact of the cathode with the corrosion electrolyte and dissolution of the cathode elements in the electrolyte. Therefore, it is expected to improve its electrochemical properties by applying LTO coating (of $Li_2Ti_3O_7$ source) on NCM523 cathode.

In this project, for the first time, purification of lithium titanate anodic material by stoichiometry $Li_2Ti_3O_7$ was performed by sol-gel method on a laboratory scale. After purification and identification of $Li_2Ti_3O_7$ (LTO) phase, its electrochemical properties such as initial capacity, cyclicity and its conductivity is measured. The cathode material $LiNi_{0.5}Co_{0.2}Mn_{0.3}O_2$ (NCM523) is then coated with $Li_2Ti_3O_7$ in weight percentages 1, 3 and 5 and the LTO coated layer is characterized

using XRD, EDS and FESEM analyzes. In the following, the effect of coating is investigated by comparing the electrochemical properties of the primary cathode with modified samples such as initial capacity, cyclic efficiency and rate capability. The effect of coating on the lithium-ion coefficient within the structure and electrochemical impedance of the battery is also studied.

2. EXPERIMENTAL SECTION

2.1. Synthesis of $Li_2Ti_3O_7$

$Li_2Ti_3O_7$ was synthesized by sol-gel method with tetrabutyl titanate $Ti(OC_4H_9)_4$ as a source of titanium and lithium hydroxide LiOH as a source of lithium. Thus, first the stoichiometric amount of tetrabutyl titanate was dissolved in isopropyl alcohol in a ratio of 1: 5. The above solution (first solution) was stirred well for 1 hour at 60 °C until a white cell was obtained using a magnetic stirrer. In the next step, a solution (second solution) containing an appropriate amount of lithium hydroxide was dissolved in a solution containing acetic acid, isopropyl alcohol and deionized water in a ratio of 1: 2: 1 and stirred with a magnetic stirrer for 2 hours. Then the second solution was added drop by drop to the first solution, at which point the color of the solution turned pale yellow. The final solution was stirred for 2 hours at 85 °C until a white gel was obtained, then dried at 120 °C to give the initial powders. The resulting powders were thermodynamically decomposed at 400 °C for 5 hours and finally calcined for 16 hours at 1100 °C to form $Li_2Ti_3O_7$ nanoparticles.

2.2. Coating of the cathodic materials

Coating of the cathode powders includes two stages of hydrolysis and lithium ionization. In hydrolysis, first a stoichiometric amount of tetrabutyl titanate was dissolved in 10 ml of pure ethanol. A mixture of pure ethanol and deionized water was then added. The solution was stirred well for 1 hour at 60 ° C until a white cell was obtained using a magnetic stirrer. The NCM powders were then added to the tube and stirred for 1 h, resulting in a titanium oxide layer forming on the NCM powders ($Li(Ni_{0.5}Co_{0.2}Mn_{0.3})O_2.xH_2O@TiO_2$). In the lithium stage, the mixture of the previous stage was first dried in an oven at 60 °C for 8 hours. The obtained powders were added to a mixture containing stoichiometric amount of lithium hydroxide and ethanol and stirred with a magnetic stirrer for 2 hours. Finally, it was calcined for 10 hours at 1100 °C to form a LTO (of $Li_2Ti_3O_7$ source) coating on the NCM powders. The Cathode powders were synthesized in three different weight percentages of one, three and five weight percent, which were named LTO1, LTO3 and LTO5, respectively. Also, to ensure the formation of lithium titanate coating, it was tested once according to the same method without adding cathode particles, which is given in the diffraction pattern.

2.3. Final electrode preparation

To perform the battery electrochemical tests, a slurry with a certain percentage of active ingredient, carbon black and polyvinylidene fluoride (PVDF) adhesive had to be prepared. For

this purpose, 80% of the synthesized electrode material, 10% by weight of carbon black and 10% by weight of PVDF were dissolved in a certain amount of N-methyl-2-pyrrolidine (NMP) solvent as follows. First, PVDF and NMP were mixed together and stirred with a magnetic stirrer for about one hour. Then the pre-dehumidified active substance (anode or cathode) and carbon black were added to the above solution and stirred for about 2-3 hours to obtain a completely viscous solution. After obtaining the cathode viscose solution, it should be placed on aluminum foil for the cathode and on copper foil for the anode, which is done using a coating and drying machine (MSK-AFA-automatic coating drying machine) and by Dr. Blade method. This coating was done automatically on aluminum foil that was completely flattened with a vacuum to achieve a uniform thickness. Finally, the lid of the device was closed and placed at 100 ° C for one hour to dry completely. Then, the foil was removed from the device, placed in it at 80 ° C overnight, and finally punched with a diameter of 13 mm.

2.4. Battery Assembly

A coin-cell battery was used for electrochemical experiments with a positive and negative electrode diameter of 13 mm and an average weight load of 2 $mg.cm^{-2}$. Lithium metal is also used as the anode, and the separator in the battery is a porous polypropylene (pp) plate. Also, the electrolyte is a standard molar solution of lithium hexafluorophosphate ($LiPF_6$) in a mixture of ethylene carbonate (EC) and dimethyl carbonate (DMC) in a ratio of 1: 1, which forms HF acid in the presence of moisture. The process of making the battery was done by placing the electrode on the positive side of the 2032 size coin cell.

2.5. Measurements

X-ray diffraction was performed to identify and study the crystal structure of the electrodes using an XRD device made by Rigaku of Japan. In this analysis, Cu-kα beam irradiation with scanning rate of 2 seconds per degree between angles (2θ) of 10-90 degrees was used. The morphology of the anodic material, the primary cathode and coated with lithium titanate was examined using a field emission scanning electron microscope (FESEM). Electrochemical and battery performance tests were performed with 4000BTS battery tester manufactured by Neware China.

3. RESULTS AND DISCUSSION

3.1. Material Characterization

Because of that, $Li_2Ti_3O_7$ is stable at temperatures above 900 °C, when calcined at high temperatures, the lithium source is reduced, leaving the remaining titanium as titanium oxide (anatase phase) in the final material [34]. Therefore, in order to achieve stoichiometry with the best purification result, the material was synthesized in three different Li: Ti stoichiometric ratios as 5:3, 4.4:3 and 3.6:3.

Figure 1 shows the diffraction pattern for lithium titanate ($Li_2Ti_3O_7$) without any impurity phase. XRD patterns of this sample with the best purification result includes titanium-containing precursor (tetrabutyl titanate: $Ti(OC_4H_9)_4$) (Li)4.4:(Ti)3 show a well-crystallized Ramsdellite structure with the P_{bnm} spatial group. Based on the obtained peaks, the structure obtained for $Li_2Ti_3O_7$ is orthrombic with spatial group Pbnm-62.

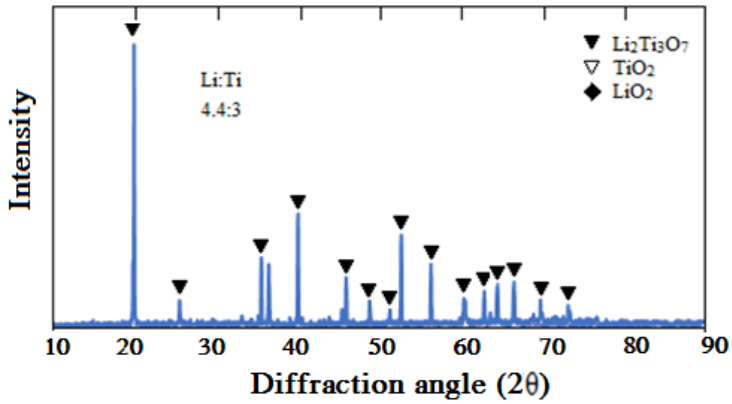

Figure 1. X-ray diffraction pattern of $Li_2Ti_3O_7$ synthesized with the best purification result includes (Li)4.4:(Ti)3

As a result, according to the XRD identification card (00-035-0126), it is observed that in the synthesis method with the ratio of lithium to titanium precursor, 4.4 to 3, respectively, no impurity phase is formed and the resulting pattern is completely in accordance with $Li_2Ti_3O_7$ stoichiometry [35,36].

FESEM images of lithium titanate in various magnifications are shown in Figures 2. As seen, lithium titanate is composed of small, 20-nanometer medium-sized particles which agglomerate to form larger particles in the range of 50 nm to 1 μm. Smaller particles are generally spherical and agglomerated particles are irregular in shape.

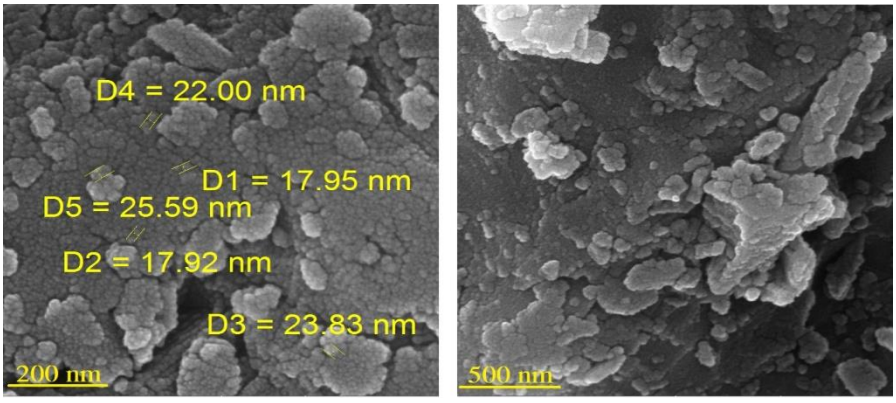

Figure 2. FESEM images of lithium titanate $Li_2Ti_3O_7$ at 200 and 500 nm magnification in two different regions

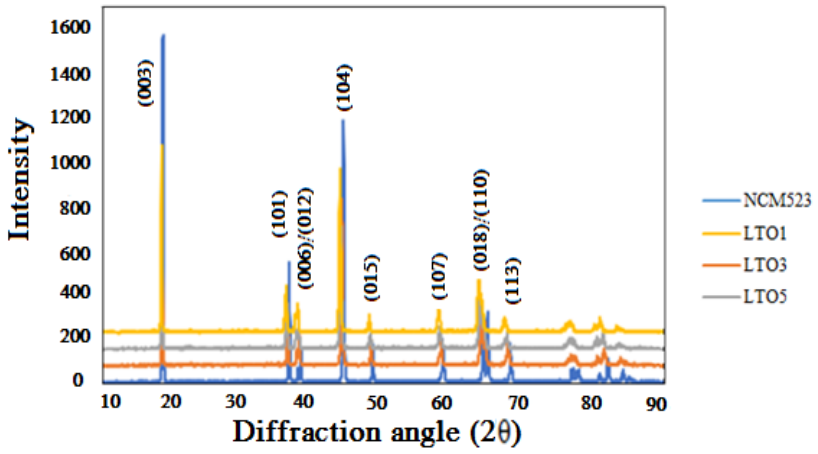

Figure 3. X-ray diffraction pattern for the primary cathode and coated with a different weight percentage of lithium titanate

Figure 3 shows the X-ray diffraction pattern for the initial and coated $Li(Ni_{0.5}Co_{0.2}Mn_{0.3})O_2$ cathode with various amounts of lithium titanate. All XRD patterns of the samples show the hexagonal structure of α-$NaFeO_2$ with the spatial group R3m. The (012) / (006) and (110) / (018) peaks are clearly distinct from each other, indicating that all specimens have a layered structure. No additional peak of $Li_2Ti_3O_7$ was observed, which may be due to the small amount of this phase. It also indicates that the coating method did not result in a secondary phase or impurity in the cathode material. Using these patterns, the lattice parameters and the intensity ratio of (104) / (003) peaks were calculated for each sample, which is given in Table 1. As can be seen, the lattice parameter and the internal distance of the plate (003) of the samples increased with increasing weight percentage of LTO coating, which is due to the replacement of some Ti^{+4} (0.605 Å) ions with smaller Co^{3+} (0.545 Å) or Mn^{+4} (0.53 Å) ions within the NCM523 layer structure.

Table 1. Lattic parameters and plate spacing and peak intensity ratio (003)/(104) for prototype and coated samples

Peak intensity ratios (003)/(104)	**Plate (003) spacing (Å)**	**Lattic parameters**			**Sample**
		c/a (Å)	c (Å)	a (Å)	
1.321	4.719	4.950	14.207	2.870	**NCM523**
1.336	4.757	4.953	14.214	2.870	**LTO1**
1.288	4.761	4.956	14.235	2.872	**LTO3**
1.391	4.776	4.956	14.263	2.878	**LTO5**

The mixing of cations within the layered oxide network is determined by the peak intensity ratio of (003)/(104), so that if the peak intensity ratio of (003)/(104) is less than 1.2, it indicates the high degree of mixing of cations due to the occupation of foreign ions [36]. The peak intensity ratio of (003)/(104) for all samples was calculated to be greater than 1.2, which indicates the low mixing of cations.

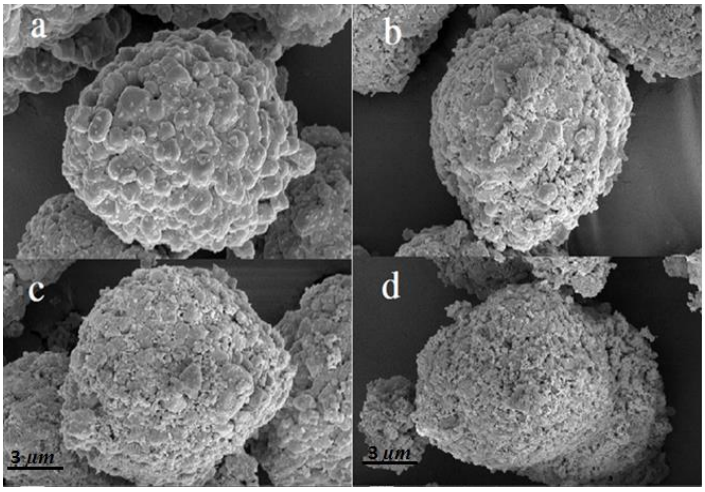

Figure 4. FESEM image of samples a) NCM523, b) LTO1, c) LTO3 and d) LTO5 in 3 micrometers of magnification

Figure 4 shows the FESEM image of the morphology and microstructure of the initial $Li(Ni_{0.5}Co_{0.2}Mn_{0.3})O_2$ and LTO1, LTO3, LTO5 coated cathodes in 3µm magnifications. As can be seen, the morphology of NCM523 and the coated specimens are different, indicating that the coating method had an effect on the morphology of the primary powders. As shown in Figure 4-a, NCM particles have a smooth surface without any layer of coating. The NCM is also a multidimensional structure with particles about 200-500 nm in size, which stick together and form spherical particles about 3 micrometers in size. The morphology of the cathode material is strongly correlated with the electrochemical properties of the lithium-ion battery.

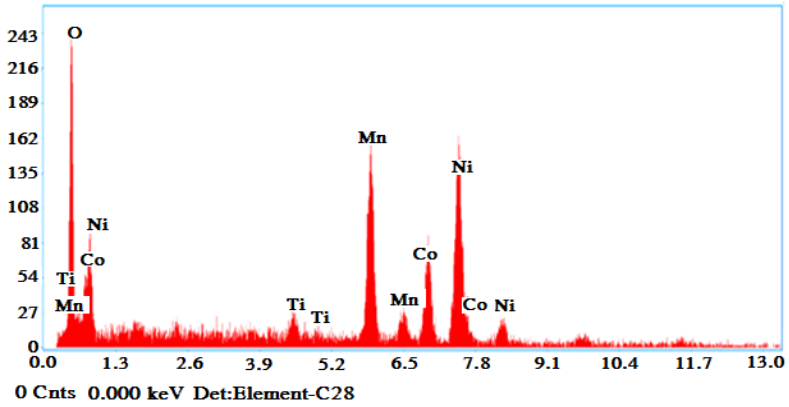

Figure 5. EDS Diagram of cathode with 3% lithium titanate coating

Particle distribution and material uniformity provide good performance during charging / discharging. As can be seen in the images of the modified specimens (Figure 4-b, c and d), after coating, the surface of the specimens has become rough and some nanometer particles have formed like villi. These particles are most evident in the LTO5 sample. In addition to FESEM images, X-ray energy distribution (EDS) spectroscopy was performed to determine the presence of different elements for the LTO3 sample. Figure 5 shows the EDS spectrum of the cathode with a 3% coating of lithium titanate along with the identification of an element whose Ti presence is visible alongside the rest of the cathode elements in the EDS. The data were compared to investigate the microstructural properties and it was found that the internal ratio of Ni, Co and Mn elements in the coated sample is the same ratio of 5: 2 to 3 that can be measured in the prototype. These data show that the coating method had no effect on the initial cathode composition. The weight percentages and atomic percentages of Ni, Mn, Co, O and Ti for LTO3 are given in Table 2.

Table 2. Percentage of elements in NCM coated with 3% wt LTO

Atomic percentage (%)	Weight percentage (%)	Atomic number	Elements
35.9	13.5	8	**O**
2.3	2.6	22	**Ti**
20.2	26.1	25	**Mn**
12.7	17.6	27	**Co**
28.8	39.9	28	**Ni**

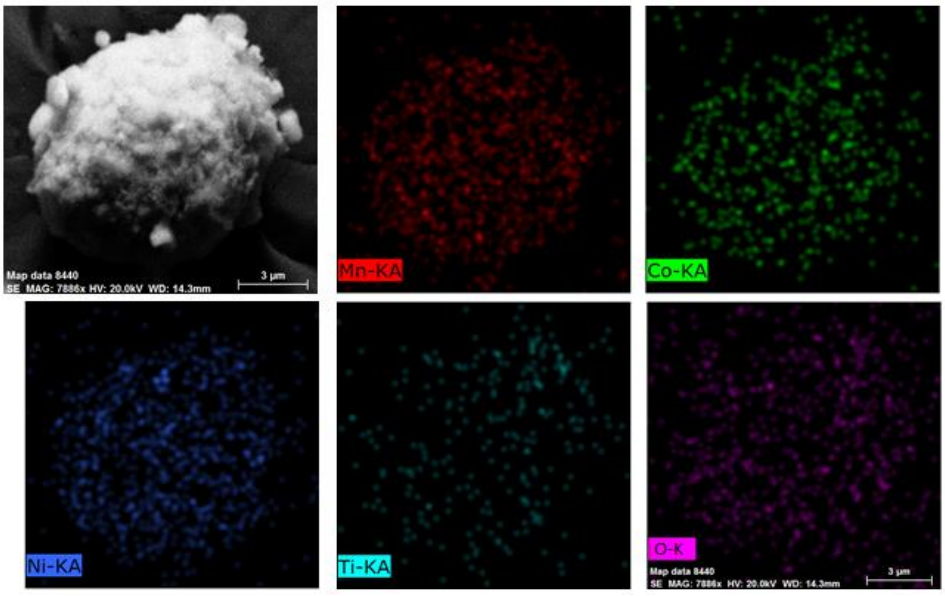

Figure 6. EDS mapping analysis of LTO3 samples for Ni, Mn, Co, O and Ti elements

Figure 6 also shows the EDS mapping analysis of LTO3 cathode for Ti, Ni, Co, Mn and O. As can be seen, the elements Ti, Ni, Co, Mn and O are evenly distributed on the surface of the coated cathode. Also, due to the uniform distribution of Ti on the cathode surface, it can be assumed that the LTO coating evenly covers the cathode surface. According to the HRTEM images (Figure 7 red lighted) clearly shows that a relatively uniform and thin coating layer exists on the surface of NCM523, and the thickness of the coating layer is approximately 2 nm.

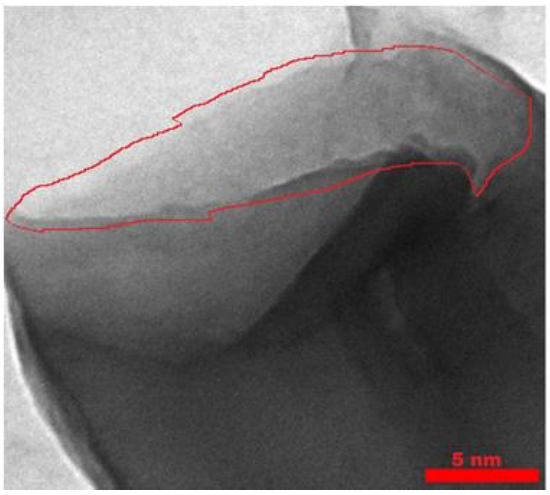

Figure 7. HRTEM image of LTO3 with 3% lithium titanate coating

3.2. Electrochemical Performance

The initial charge-discharge curve of the uncoated and coated samples at cut-off discharge voltage equal to 2.5 and cut-off charge voltage equal to 4.3 V and the charge-discharge rate of 0.2 C are shown in Figure 8. As can be seen, the curved shape of all the samples is similar to each other. Also, all electrodes showed a flat potential of 3.7 volts, which means that LTO coating had no effect on the intrinsic properties of the NCM cathode such as crystal structure but influenced the charge-discharge behavior and the electrochemical performances [37]. The discharge capacities of NCM, LTO1, LTO3 and LTO5 at the rate of 0.2 C are 165.3, 169.5, 179.2 and 172.3 mAh / g, respectively. The increase in the discharge capacity of the modified samples compared to the discharge capacity of the uncoated sample is due to the fact that the LTO coating acts as additional sites for the insertion of lithium ions [36]. Discharge capacity of LTO5 is lower than discharge capacity of LTO3, which indicates that with increasing the weight percentage of the coating and increasing the thickness of the coating, the insrtion / desertion of lithium ions to the electrode structure becomes more difficult and the coating acts as a barrier to lithium-ion diffusion. The Coulombic efficiency, defined as the ratio of discharge capacity to charge capacity, is 89.8%, 92.5%, 95.6% and 93.5% for NCM, LTO1, LTO3 and LTO5, respectively. The increase in Coulombic efficiency in the coated samples may be due to the fact that the release of oxygen as Li_2O from the layered lattic in the high potential region has been reduced or reached to zero [34]. For the modified samples, at the end of the discharge

process, it is observed that the potential decreases with a steeper slope than for the uncoated sample, which suggests that the polarization of the electrodes is reduced after LTO coating with $Li_2Ti_3O_7$. Also, the irreversible capacity in the coated samples is less than the prototype, which indicates that the polarization and internal resistance of the cell, including the modified samples, is less [38].

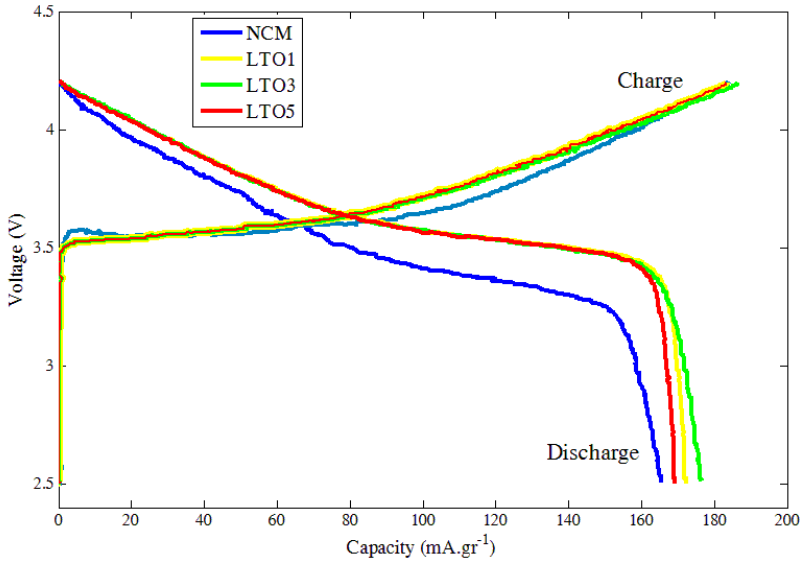

Figure 8. Initial charge-discharge diagram for NCM523 cathode and coated with different percentage of lithium titanate at the rate of 0.2 C and charge and discharge voltage cut-off equal to 4.3 and 2.5 volts, respectively

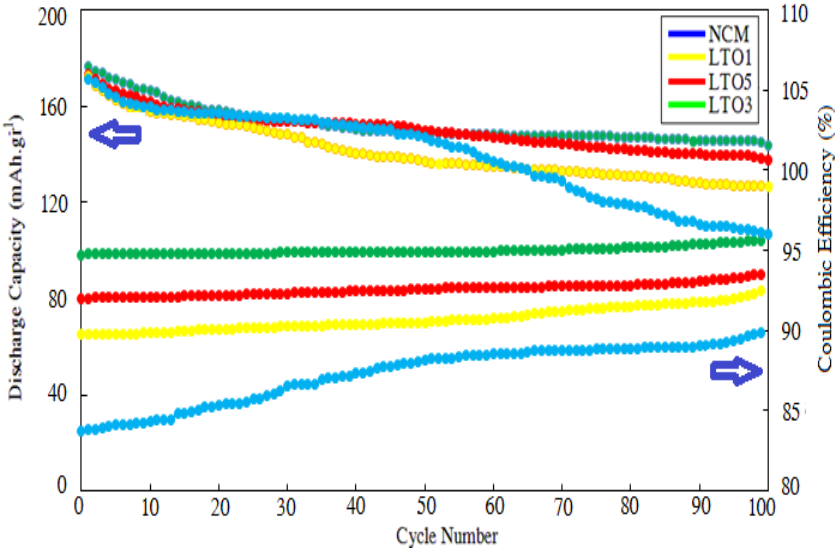

Figure 9. Cyclic performance of NCM523 cathode and coated with different percentage of lithium titanate at 1C rate

Also, some Ti^{+4} ions are doped into the structure of the primary cathode, which increases its electrochemical activity [38]. The values of the initial discharge and charge capacity, irreversible capacity and Coulombic efficiency for the prototype and coated are given in Table 3. Discharge

capacity diagram in different cycles for the uncoated and coated samples are shown in Figure 9. As can be seen, all cathodes have a capacity drop after 100 cycles, but the diagrams for the modified materials showed more stability in the discharge capacity during the cycles than the original cathode. The initial discharge capacity of NCM, LTO1, LTO3 and LTO5 samples at C1 rate is 153.9, 159.3, 172.1 and 163.8 mAh/g, respectively, which like the previous part, the capacity of the coated samples are higher than the uncoated samples due to the active coating. The discharge capacity of NCM, LTO1, LTO3 and LTO5 samples after 100 cycles is 89.5, 114.1, 163.1 and 139.5 mAh/g, respectively, and the percentage of remaining capacity of the samples is 58.2, 71.6, 94.8 and 85.1% respectively. Improving the cyclic performance of the samples which modified with LTO coating is due to the fact that the applied coating prevents direct contact of the NCM cathode with the LiPF6 electrolyte and its dissolution in the electrolyte components specially includes HF.

Table 3. Electrochemical data related to the initial charge / discharge process for the bare $LiNi_{0.5}Co_{0.2}Mn_{0.3}O_2$ cathode and coated with different amounts of Li-Ti-O at rate of 0.2 C and voltage range of 2.5 -4.2 V

Initial columbic (%) efficiency	**Irreversible (mAh/g) capacity**	**Initial charge (mAh/g) capacity**	**Initial discharge (mAh/g) capacity**	**Cathode**
89.8	18.8	184.1	165.3	**NCM523**
92.5	13.8	183.3	169.5	**LTO1**
95.6	10.1	186.3	179.2	**LTO3**
93.5	11.9	184.2	172.3	**LTO5**

In the other words, The LTO coating layer can not only suppress the side reaction between the electrolyte and the surface of the NCM particles, but also improve the structural stability of NCM. As a result, the formation of interphase solid electrolyte (SEI) is delayed [39]. Also, doping of Ti^{4+} inside the cathode structure will improve the structural stability of the coated cathode compared to the uncoated cathode [40]. In the coated samples, it can be seen that the LTO3 sample had the best cyclic performance. In the LTO5 sample, due to the increase in coating thickness, it showed less capacity than the LTO3 sample after the end of 100 cycles. Also, in LTO1 sample, it is thought that due to the low thickness of the coating, the coating will be corroded sooner than other samples, therefore it has the weakest performance in cyclic stability, although it is much more stable and with more capacity than the sample without coating. Therefore, according to the references, the electrochemical performance and the capacity retention of the LTO3, at 1C after 100 cycles are better (94.8%) than the similar recent works based on the bare NCM523 such (64.3% [20]), (84.3%

[34]), (80% [39]) and also than the similar works based on the NCM811 such (88.6% [11]), NCM0.9,0.05,0.05 such (91% [12]), and NCA such (90.8% [7]).

The performance of the prototype and coated samples at different rates from 0.2 to 10C and at each rate, 5 cycles at ambient temperature were evaluated. The results of this test are shown in Figure 10. As can be seen, at all rates, the coated samples showed a higher capacity than the uncoated sample. Medium cathode discharge capacity without coating at rates C (0.2-1-2-5-10) were obtained 160.4, 154.1, 138.9, 85.5, 39.5 mAh per gram respectively; While these values are for the LTO3 sample were obtained 176.5, 171.8, 148.2, 103.8, 74.7 mAh/g respectively. As can be seen, the difference between the uncoated sample and the coated sample is more pronounced at high discharge rates such as C5 and C10. At C10, the average discharge capacity of NCM, LTO1, LTO3 and LTO5 samples were 39.5, 61.2, 74.2 and 69.7 mAh/g, respectively. At high charge-discharge rates, the insertion / removal of lithium ions should be done quickly, so it is better to have a high lithium ion penetration coefficient or a short lithium ion penetration path [41].

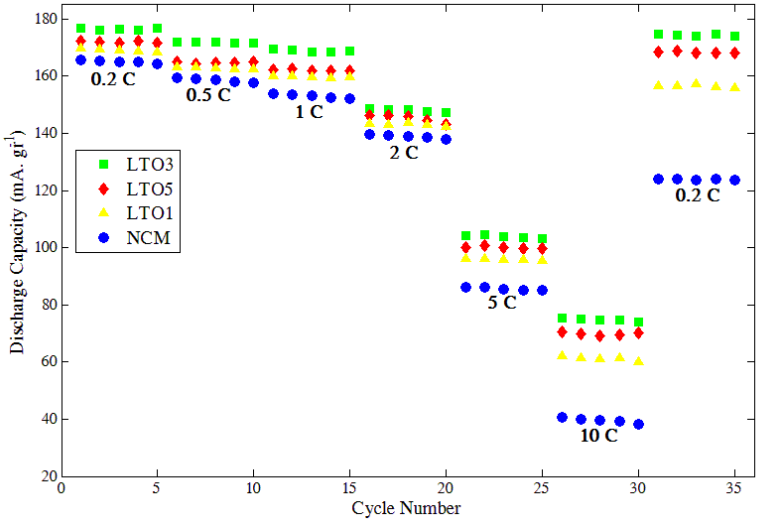

Figure 10. Rate capability of NCM523, LTO1, LTO3 and LTO5 samples at different discharge rates at room temperature

As further electrochemical impedance experiments will show, the diffusion coefficient of lithium ions inside the modified cathodes is much higher than the prototype, so the discharge capacity of the modified samples at the C10 discharge rate is much higher than the prototype. When the charge-discharge rate is returned to the original rate of 0.2, it is observed that the residual capacities of the NCM, LTO1, LTO3 and LTO5 samples are 123.9, 156.6, 174.3 and 168.2, respectively. It was found that about 77%, 92%, 99% and 97% of the initial capacity are at the same rate, respectively. To better show the effect of the coating on the cathode at different discharge rates, the average discharge capacity of NCM and LTO3 samples at each rate was normalized to their corresponding initial discharge capacity at 0.2 C discharge rate. As shown in Figure 11, it is clear

that the modified LTO3 sample has a higher capacity than the uncoated sample. Table 4 shows the mean discharge capacity values of the samples at different discharge rates.

Table 4. Medium discharge capacities for the bare and modified samples at different charge-discharge rates

0.2	10	5	2	1	0.2	Charge-discharge rat (C)
123.9	39.5	85.5	138.9	154.1	160.4	**NCM523 (mAh/g)**
156.6	61.2	95.9	143.1	159.9	169.2	**LTO1 (mAh/g)**
174.3	74.7	103.8	148.2	168.9	176.5	**LTO3 (mAh/g)**
168.2	69.7	100.1	145.2	162	171.9	**LTO5 (mAh/g)**

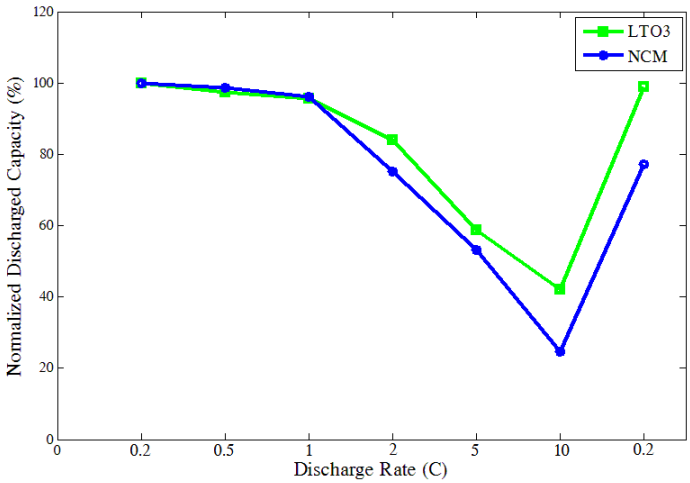

Figure 11. Normalized discharge capacity diagram of LTO3 and NCM523 samples relative to the initial discharge capacity

To investigate the effect of LTO coating layer on internal resistance and mobility of lithium ions, electrochemical impedance spectroscopy (EIS) of NCM523, LTO1, LTO3 and LTO5 samples after 5 cycles at 1C charge-discharge rate and cut-off discharge-charge voltages equal to 2.5 and 4.3 V was performed. Figure 12 shows the electrochemical impedance spectroscopy (EIS) of lithium titanate-coated primary cathode materials with obvious differences in the resistance of the coated and uncoated. The relevant equivalent circuits corresponding to the Nyquist diagrams of the specimens are similar. In the equivalent circuit, R_s indicates the internal ohmic resistance, which includes the resistance of the electrolyte and other resistive components, and its value is equal to the intersection of the diagram with the true Z axis at high frequency. R_{sf} corresponds to the resistance

of the surface film at high frequencies and the first semicircle due to the formation of an insulating layer at the electrolyte interface or the decomposition of organic components at the electrode surface. R_{ct} corresponds to the charge transfer resistance that corresponds to the second semicircle in the low frequency range. The R_{sf} value in the uncoated sample increases sharply with increasing cycle. While in the sample coated with 3% by weight, it remains almost constant, indicating that the interfacial solid electrolyte (SEI) layer is stable throughout the cycles. In the Nyquist diagram, the oblique line which seen in the low frequency region, is related to the transfer of lithium ions in the solid phase, the slope of which indicates the Warburg impedance (W) [42].

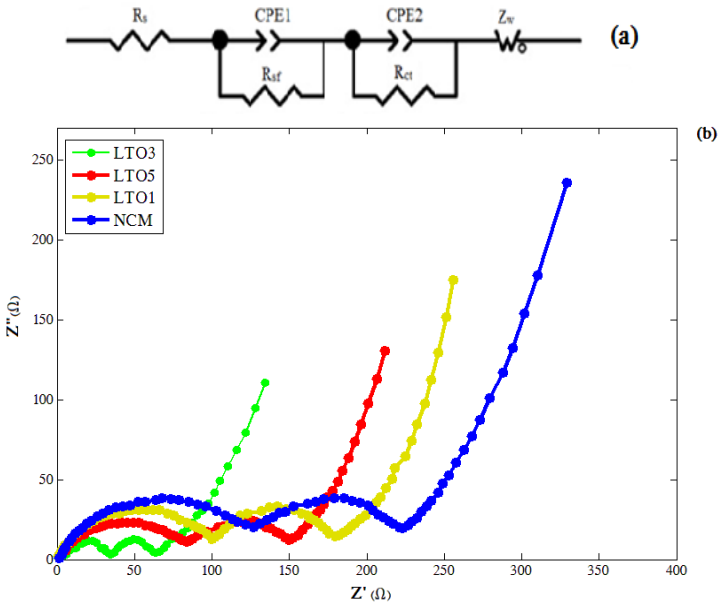

Figure 12. a) Equivalent circuit of the Nyquist diagram, b) Imaginary impedance diagram in terms of real impedance of the prototype and coated samples after 5 charge-discharge cycles at rate of 1C

As it is known, the charge transfer resistance for the coated sample is much lower than the uncoated sample, which is due to the easier transfer of electrons on the surface of the modified cathodes due to the higher electrical conductivity of the coated samples. The charge transfer resistors for NCM523, LTO1, LTO3 and LTO5 were obtained 118.7, 74.9, 30.7 and 64.6 ohm, respectively. Also, the surface film resistance in coated samples was decreased, which measured for NCM523, LTO1, LTO3 and LTO5 samples as 99.48, 83.91, 26.92 and 61.61 ohms, respectively. These observations show that the LTO layer reduces the barriers to lithium-ion transfer at the electrode-electrolyte interface. The coating layer also facilitates and accelerates the transfer of lithium ions in the interface by creating a three-dimensional path for the transfer of lithium ions. As shown in the electrochemical experiments, at high charge-discharge rates, what improves the rate efficiency of the coated cathode is due to this high ionic conductivity of the LTO coating (of $Li_2Ti_3O_7$ source) [43].

Also, with increasing the coating thickness from 3% by weight to 5%, it is observed that the values of surface film resistance and charge transfer have increased due to the increase in the penetration path in the process of intercalation/deintercalation of lithium ions.

Table 5. Surface film resistance, charge transfer resistance and lithium-ion diffusion coefficient of NCM523, LTO1, LTO3 and LTO5 samples

D_{Li+} ($cm^2\ s^{-1}$)	R_{ct} (±Ω)	R_{sf} (±Ω)	R_s (±Ω)	Samples
4.1×10^{-11}	118.70	99.48	5.36	**NCM523**
5.2×10^{-11}	74.90	83.91	3.56	**LTO1**
9.7×10^{-11}	30.70	26.92	1.89	**LTO3**
5.7×10^{-11}	64.60	61.61	3.42	**LTO5**

In order to investigate the effect of lithium titanate coating on the conductivity of lithium ion, the diffusion coefficient of lithium ion in the electrode is calculated. Figure 13 shows the Z_{real} curve in terms of $\omega^{(-1/2)}$. The values obtained for the diffusion coefficient of lithium ions are given in Table 5. As can be seen, with increasing R_{ct}, the diffusion coefficient of lithium-ion decreases. These results show that the conductive layer of $Li_2Ti_3O_7$ protects the electrode particles from degradation, which improves the electron transfer.

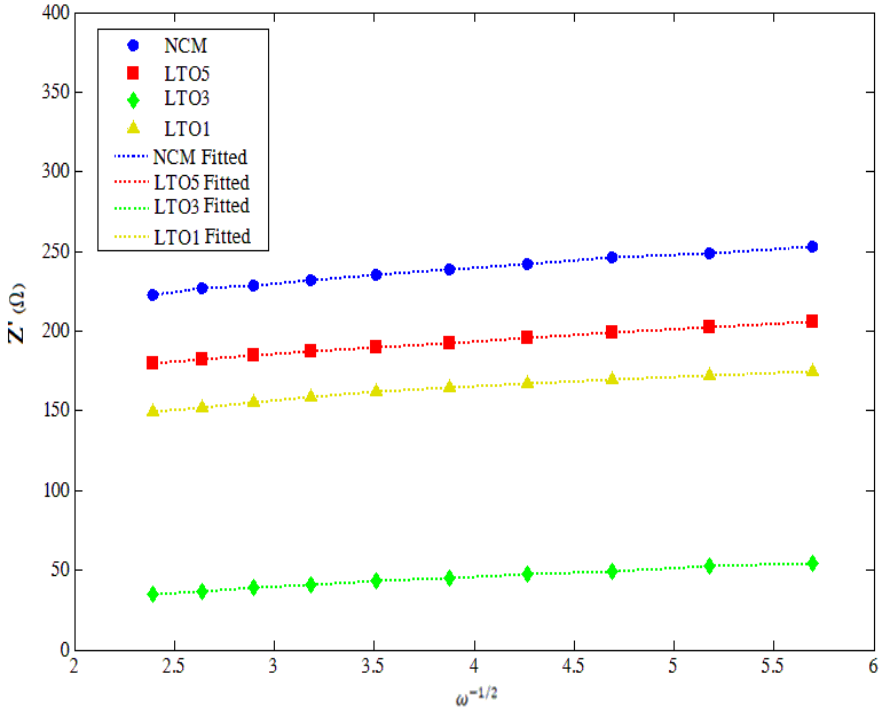

Figure 13. Real impedance diagram in terms of $\omega^{(-1/2)}$ of prototypes and coated samples after 5 charge-discharge cycles at rate of 1C

4. CONCLUSION

According to the XRD data, the lithium titanate compound was synthesized purely. Also, the crystal structure of the cathode did not change much before and after the coating process. No impurities and secondary phases and no additional LTO-related peaks were observed in the modified samples. Fixed lattice values and plate spacing (003) increased slightly with increasing weight percentage of LTO coating due to the penetration of titanium into the cathode structure.

Field-emission scanning electron microscopy (FESEM) images showed that the coating method had effect on the morphology and particle size of NCM523.

EDS analysis showed that titanium was evenly distributed on the cathode surface. It was also found that the internal ratio of the cathode elements namely Ni, Co and Mn in all samples is the same ratio of 5: 2 to 3.

The initial charge-discharge curve for all samples, which was performed at cut-off voltage of 4.3-2.5V and a discharge rate of 0.2 C, showed an increase in the initial discharge capacity of the coated samples compared to the prototype. Discharge capacity of NCM523, LTO1, LTO3 and LTO5 samples were 165.3, 169.5, 179.2 and 172.3 mAh/g, respectively.

The columbic efficiency of the coated samples was higher than that of the original cathode due to the role of the coating in preventing the release of oxygen as Li_2O. These values were calculated for NCM523, LTO1, LTO3 and LTO5 samples were 89.8%, 92.5%, 95.6% and 93.5%, respectively.

With performing the cyclability test at C1, it was found that the coated samples showed a much higher capacity than the prototype after 100 charge-discharge cycles. These values for NCM523, LTO1, LTO3 and LTO5 samples were 89.5, 114.1, 163.1 and 139.5 mAh /g, also the percentage of remaining capacity were obtained 58.2, 71.6, 94.8 and 85.1 respectively.

The improved cyclability of the modified sample LTO than the bare and recent published nickel-riched cathode material is due to the prevention of contact of the cathode material with the electrolyte and the reduction of its dissolution in the electrolyte. Also, with calculating the diffusion coefficient of lithium ion inside the structure of the primary and modified cathodes, it was shown that LTO coating increased the diffusion coefficient of lithium ion in the coated samples.

REFERENCES

[1] W. Cho, Y.J. Lim, S. M. Lee, J.H. Kim, J.-H. Song, J. S. Yu, Y. J. Kim, and M. S. Park, ACS Appl. Mater. Interfaces 45 (2018) 38915.

[2] H. Pourfarzad, M. Shabani-Nooshabadi, and M.R. Ganjali, Compos. B. Eng. COMPOS PART B-ENG. 193 (2020) 108008.

[3] N. Lebedeva, Li-ion batteries for mobility and stationary storage applications, Publications Office of the European Union (2018).

[4] S. T. Myung, F. Maglia, K. J. Park, C.S. Yoon, P. Lamp, S. J. Kim, and Y.-K. Sun, ACS Energy Lett. 2 (2017) 196.

[5] E. Zhao, M. Chen, Z. Hu, D. Chen, L. Yang and X. Xiao, J. Power Sources 343 (2017) 345.
[6] Y. Yan, Three Dimensional Hybrid Nanostructures for Renewable Energy Storage Applications, UC Riverside (2018).
[7] C. L. Xu, W. Xiang, Z. G. Wu, Y. C. Li, Y. D. Xu, W.B. Hua, X. D. Guo, X. B. Zhang, and B.H. Zhong, J. Alloys Compd. 740 (2018) 428.
[8] H. Wu, Z. Wang, S. Liu, L. Zhang, and Y. Zhang, Chem. Electro. Chem. 2 (2015) 1921.
[9] L. Tian, H. Yuan, Q. Shao, S.D.A. Zaidi, C. Wang, and J. Chen, Ionics 26 (2020) 4937.
[10] W. Xiang, W. Y. Liu, J. Zhang, S. Wang, T. T. Zhang, K. Yin, X. Peng, Y. C. Jiang, K.H. Liu, and X. D. Guo, J. Alloys Compd. 775 (2019) 72.
[11] P. Hou, J. Yin, M. Ding, J. Huang, and X. Xu, Small 13 (2017) 1701802.
[12] K.J. Park, H.G. Jung, L.Y. Kuo, P. Kaghazchi, C.S. Yoon, and Y.K. Sun, Adv. Energy Mater. 8 (2018) 1801202.
[13] Y. K. Sun, Z. Chen, H. J. Noh, D. J. Lee, H. G. Jung, Y. Ren, S. Wang, C.S. Yoon, S. T. Myung, and K. Amine, Nat. Mater. 11 (2012) 942.
[14] H. Chen, M. Ling, L. Hencz, H.Y. Ling, G. Li, Z. Lin, G. Liu, and S. Zhang, Chem. Rev. 118 (2018) 8936.
[15] F.A. Susai, H. Sclar, Y. Shilina, T.R. Penki, R. Raman, S. Maddukuri, S. Maiti, I.C. Halalay, S. Luski, and B. Markovsky, Adv. Mater. 30 (2018) 1801348.
[16] S. Kalluri, M. Yoon, M. Jo, H.K. Liu, S.X. Dou, J. Cho, and Z. Guo, Adv. Mater. 29 (2017) 1605807.
[17] Z. Chen, Z. Wang, G. T. Kim, G. Yang, H. Wang, X. Wang, Y. Huang, S. Passerini, and Z. Shen, ACS Appl. Mater. Interfaces 11 (2019) 26994.
[18] L. Zhao, G. Chen, Y. Weng, T. Yan, L. Shi, Z. An, and D. Zhang, J. Chem. Eng. 401 (2020) 126138.
[19] T. Liu, S. X. Zhao, K. Wang, and C. W. Nan, Electrochim. Acta 85 (2012) 605.
[20] M. Zhang, G. Hu, L. Wu, Z. Peng, K. Du, and Y. Cao, Electrochim. Acta 232 (2017) 80.
[21] K. Yang, L. Z. Fan, J. Guo, and X. Qu, Electrochim. Acta 63 (2012) 363.
[22] M.R. Laskar, D.H. Jackson, S. Xu, R.J. Hamers, D. Morgan, and T.F. Kuech, ACS Appl. Mater. Interfaces. 9 (2017) 11231.
[23] M. Dong, Z. Wang, H. Li, H. Guo, X. Li, K. Shih, and J. Wang, ACS Sustain. Chem. Eng. 5 (2017) 10199.
[24] Y. Chen, Y. Li, W. Li, G. Cao, S. Tang, Q. Su, S. Deng, and J. Guo, Electrochim. Acta 281 (2018) 48.
[25] H. Chen, L. Xiao, P. Liu, H. Chen, Z. Xia, L. Ye, and Y. Hu, Ind. Eng. Chem. Res. 58 (2019) 18498.
[26] Z. Li, H. Zhao, P. Lv, Z. Zhang, Y. Zhang, Z. Du, Y. Teng, L. Zhao and Z. Zhu, Adv. Funct. Mater. 28 (2018) 1605711.

[27] J. Shi, Y. Liang, L. Li, Y. Peng, and H. Yang, Electrochim. Acta 155 (2015) 125.
[28] A.L. Narayana, M. Dhananjaya, N.G. Prakash, O. Hussain, and C. Julien, Ionics 23 (2017) 3419.
[29] F. Chen, R. Li, M. Hou, L. Liu, R. Wang ,and Z. Deng, Electrochim. Acta 51 (2005) 61.
[30] P. Díaz-Carrasco, P.M. Ferreira, O. Dolotko, J. Pérez-Flores, U. Amador, A. Kuhn, and F. García-Alvarado, J. Mater. Sci. 51 (2016) 4520.
[31] S. Garnier, C. Bohnke, O. Bohnke, and J. Fourquet, Solid State Ion 83 (1996) 323.
[32] G. Li, X. Feng, Y. Ding, S. Ye and X. Gao, Electrochim. Acta. 78 (2012) 308.
[33] Z. Wang, S. Huang, B. Chen, H. Wu, and Y. Zhang, J. Mater. Chem. 2 (2014) 19983.
[34] J. Wang, Y. Yu, B. Li, T. Fu, D. Xie, J. Cai, and J. Zhao, Chem. Phys. Chem. 17 (2015) 32033.
[35] T. F. Yi, J. Shu, Y. R. Zhu, A. N. Zhou, and R. S. Zhu, Electrochem. commun. 11 (2009) 91.
[36] H. Deng, P. Nie, H. Luo, Y. Zhang, J. Wang, and X. Zhang, J. Mater. Chem. 2 (2014) 18256.
[37] Z. Chen, Y. Qin, K. Amine, and Y. K. Sun, 20 (2010) 7606.
[38] J. Lu, Q. Peng, W. Wang, C. Nan, L. Li and Y. Li, and J. Am. Chem. Soc. 135 (2013) 1649.
[39] Y. Mo, B. Hou, D. Li, X. Jia, B. Cao, L. Yin, and Y. Chen, RSC Adv. 6 (2016) 88713.
[40] A. Zhou, X. Dai, Y. Lu, Q. Wang, M. Fu, and J. Li, ACS Appl. Mater. Interfaces 8 (2016) 34123.
[41] L. Li, Z. Chen, L. Song, M. Xu, H. Zhu, L. Gong, and K. Zhang, J. Alloys Compd. 638 (2015) 77.
[42] J. Z. Kong, C. Ren, Y. X. Jiang, F. Zhou, C. Yu, W. P. Tang, H. Li, S. Y. Ye, and J. X. Li, J. Solid State Electrochem. 20 (2016) 1435.
[43] Y. Cao, S. Cai, S. Fan, W. Hu, M. Zheng, and Q. Dong, Faraday Discussions 172 (2014) 215.